General Biology

AGING EFFECTS ON CORTICAL NETWORK CONNECTIVITY DURING SPEECH PERCEPTION IN NOISE: A GRAPH THEORETICAL ANALYSIS

John P. Sheppard[1,3,+], Ji-Ping Wang[2], Patrick C.M. Wong[3,4,5,6,*]

[1]Department of Biomedical Engineering/[2]Department of Statistics/[3]Roxelyn & Richard Pepper Department of Communication Sciences and Disorders/[4]Northwestern University Interdepartmental Neuroscience Program/[5]Hugh Knowles Center/[6]Department of Otolaryngology—Head and Neck Surgery/ Northwestern University, Evanston, IL, 60208, United States

Introduction: Traditional fMRI data analyses such as the general linear model (GLM) have been useful in capturing regional activation associated with behavioral responses, but fall short in characterizing brain network properties. Following recent research that has elucidated characteristic network topologies recurrent across diverse types of complex systems, we applied graph theory to model the human cerebral cortex as a functional network composed of nodes with functional connections or links. Cerebral hemodynamic (functional) data were taken from our previous study examining the effects of aging on speech perception in noise. We examined network parameters including degree (number of links possessed by a single node), clustering coefficient (fraction of actual versus potential links between neighbors of a node), and efficiency (relative speed of information transfer defined as the inverse of the harmonic mean of shortest path lengths), and tested the hypothesis that younger adults' capacity for more accurate speech perception in noise is associated with more robust network connectivity when compared to older adults.

Methods: Post-processing of MR imagine data consisted of motion and slice-timing correction, spatial smoothing, resampling to $6mm^3$ resolution and transformation to a common atlas of the brain. Voxel time series data of the cortical grey matter were then extracted and analyzed for network connectivity. Global network data such as degree distribution, average node degree, network clustering coefficient and efficiency were calculated as well as voxel-wise parameters including degree, clustering coefficient, and efficiency of each node. Normalized measures were obtained by comparing network measures to those in equivalent random networks. One-way ANOVAs were performed to examine group effects on network connectivity. The voxel-wise data were then projected onto anatomical scans to visualize changes in network topology across brain regions.

Results: Both young and elderly subjects possessed networks exhibiting small-world characteristics, and demonstrated exponentially-truncated power-law degree distributions (as networks became more sparse at higher thresholds, some networks displayed scale-invariant topologies). Younger subjects were found to possess significantly higher average node degrees as well as significantly shorter characteristic path lengths, despite higher overall brain activation in the elderly subjects in some regions of the brain. These differences were robust across all thresholds. Nodes of exceedingly high degree were found clustered near the prefrontal cortex, precuneus, insula and auditory cortex, partially overlapping with our previous analysis based on GLM. Group effects t-tests showed specific declines in relative degree connectivity (using z-score normalization for each network), clustering and efficiency in regions of the left superior temporal gyrus (STG), including primary auditory cortex. Decreases in these measures were also observed in left inferior temporal (IT) and parahippocampal (PHG) regions.

Conclusions: The significant increases in network efficiency in younger versus older adults is consistent with the observation of shorter average path lengths in this subject group, suggesting a more efficient network in the young cortex during speech perception in noise. These findings agree with behavioral results, which found younger subjects to be significantly more accurate at identifying speech in high levels of noise. Furthermore, these data-driven graph theoretical methods corroborate with traditional hypothesis-driven methods (the GLM in our case).

Acknowledgements: J.P. Sheppard was supported by an undergraduate research grant administered through Northwestern University's Office of the Provost.

+ Corresponding author (john-sheppard@northwestern.edu)
* Faculty sponsor (pwong@northwestern.edu)

Appendix I: References

Achard, S. et al. (2006) A Resilient, Low-Frequency, Small-World Human Brain Functional Network with Highly Connected Association Cortical Hubs. *J. Neurosci.* 26(1): 63-72.

Barabasi, A.L. (2004) Network biology: Understanding the cell's functional organization. *Nature Reviews Genetics*, 5:101-113.

Bullmore, E. & Sporns, O. (2009) Complex brain networks: graph theoretical analysis of structural and functional systems. *Nature Reviews Neuroscience*, 10(4): 186-198.

Lijeros, F. (2001) The web of human sexual contacts. *Nature*, 411: 907-908.

Salvador, R. et al. (2005). Neurophysiological architecture of functional magnetic resonance images of human brain. *Cereb Cortex*, 15(9):1332-1342.

Sporns, O. et al. (2007). Identification and classification of hubs in brain networks. *PLoS ONE,* 2(10).

Sporns, O. & Zwi, J.D. (2004) The small world of the cerebral cortex. *Neuroinformatics*, 2: 145–162.

Watts, D.J. & Strogatz, S.H. (1998) Collective dynamics of ‘small-world’ networks*. Nature*, 393: 440–442.

Wong, P.C.M. et al. (2008) Aging and Cortical Mechanisms of Speech Perception in Noise. *Neuropsychologia*, 47: 693-703.

+ Corresponding author (john-sheppard@northwestern.edu)
* Faculty sponsor (pwong@northwestern.edu)

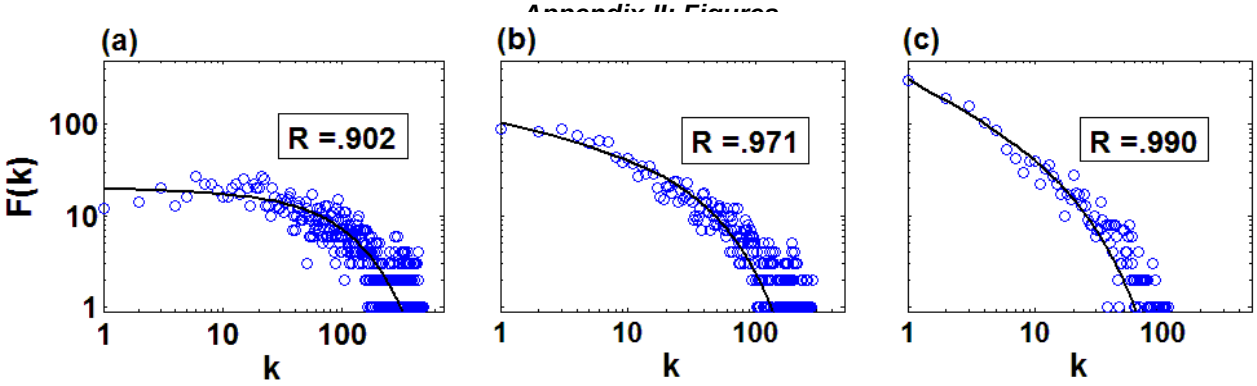

Figure 1. Degree frequency plots for networks from an elderly subject, generated at three connection thresholds under loud noise (SNR –5) listening condition. Networks exhibited exponentially-truncated power-law degree distributions with $F(k) \sim k^{-\alpha} e^{-k/kc}$. (a) $r_c = 0.6$, $\alpha = 0.026$, kc = 107; (b) $r_c = 0.7$, $\alpha = 0.328$, kc = 109; (c) $r_c = 0.8$, $\alpha = 0.700$, kc = 21. Note logarithmic axes.

Group	Normalized cc	Normalized L	σ = Norm cc / Norm L
Young subjects	2.07 ± 0.306	1.34 ± 0.021	1.54 ± 0.217
Elderly subjects	1.73 ± 0.202	1.22 ± 0.034	1.40 ± 0.143

Table 1. Group averages for clustering (cc) and average path length (L) between nodes in young and elderly brain networks, demonstrating small-world characteristics. Normalized cc and L are computed by dividing the values in each network by the corresponding average value in 25 equivalent random networks. As the small world coefficient (σ) increases above unity, each network becomes more small world-like. Data shown for r_c= 0.6

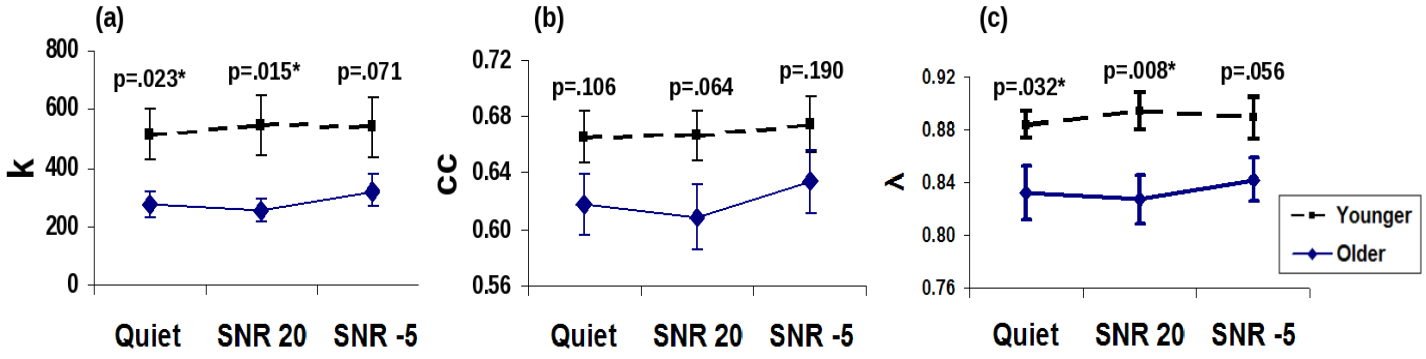

Figure 2. Group and listening condition effects on global network parameters. (a) Average node degree. Group: F(1,22) = 6.154, p = 0.021 (Young > Old); Condition: F(2,44) = 0.643, p = 0.531 ; Interaction: F(2,44) = 0.539, p = .587 (b) Clustering coefficient. Group: F(1,22) = 3.197, p = 0.088; Condition: F(2,44) = 1.725, p = 0.190 ; Interaction: F(2,44) = 0.427, p = 0.655 (c) Normalized efficiency. Group: F(1,22) = 6.538, p = 0.018 (Young > Old) ; Condition: F(2,44) = 0.694, p = 0.505 ; Interaction: F(2,44) = 1.338, p = .273. Statistics reported for mixed effects ANOVA with subject as random factor and condition as fixed within-subject factor. Error bars indicate standard error of the mean. P-values indicate results of 2-tailed, independent-sample t-tests for each condition; *

+ Corresponding author (john-sheppard@northwestern.edu)
* Faculty sponsor (pwong@northwestern.edu)

denotes significant difference ($p < 0.05$). Data shown for $r_c = 0.6$.

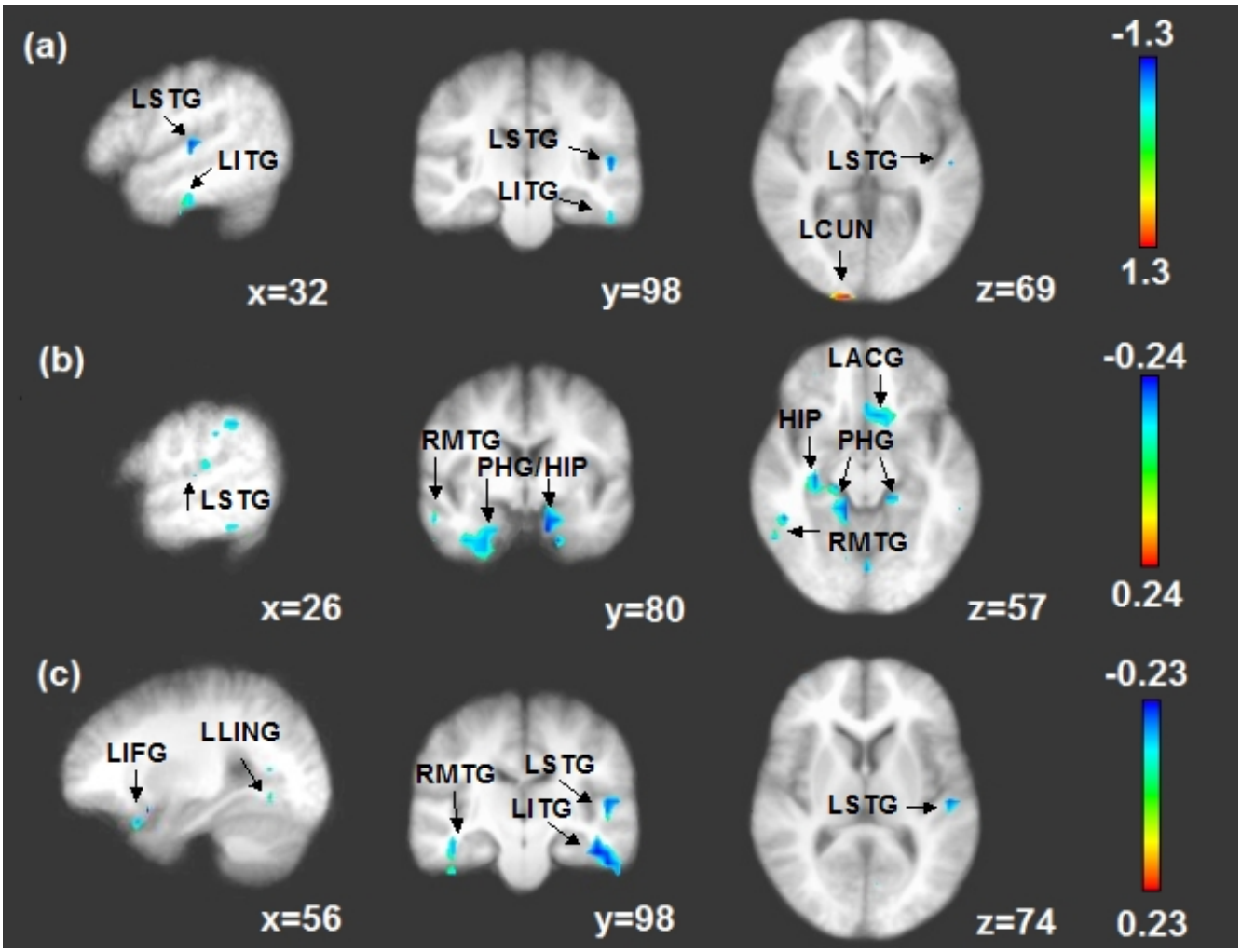

Figure 3. Left Panel (above): Brain areas showing main effect of group on (a) degree z-score, (b) clustering coefficient, and (c) normalized efficiency based on independent-sample t-tests ($p = 0.005$, uncorrected) with minimum cluster size of 2 neighboring voxels (432 mm^3). Colors represent average voxel-wise differences for each parameter (i.e. Elderly – Young; blue/red color indicate significantly higher values in young/elderly networks, respectively). Right panel (next page): List of corresponding brain regions showing cluster statistics. Data shown for $r_c = 0.6$.

+ Corresponding author (john-sheppard@northwestern.edu)
* Faculty sponsor (pwong@northwestern.edu)

Region	Peak voxel coord (mm)			Spatial extent (mm^3)	Peak T-stat	Peak significance
(a)						
RLING/17/18	-6	96	-8	2808	3.851	p < 0.001 (Old > Young)
LCUN/19	0	84	34	1296	3.420	p = 0.0025 (Old > Young)
LITG/20	48	18	-26	864	-3.689	p = 0.0013 (Young > Old)
LPHG/36/LFFG/20/37	36	36	-14	864	-4.050	p < 0.001 (Young > Old)
LSTG/22/41	48	18	10	648	-3.672	p = 0.0013 (Young > Old)
RMOG/18/19	-30	90	16	432	3.761	p = 0.0011 (Old > Young)
LMOG/18/19/LCUN	18	96	16	432	3.201	p = 0.0041 (Old > Young)
(b)						
RHIP/RFFG/RSTG/38	-24	0	-32	10800	-4.527	p < 0.001 (Young > Old)
LPHG/LHIP/LAMYG*	12	6	-20	6264	-4.937	p < 0.001 (Young > Old)
RFFG/RITG/20	-60	24	-26	1512	-3.573	p = 0.0017 (Young > Old)
LFFG/LITG/20/36	48	36	-26	1512	-3.742	p = 0.0011 (Young > Old)
LPHG/30/35	12	30	-8	1296	-3.532	p = 0.0019 (Young > Old)
LIPL/40/LSMG	54	36	40	1296	-3.400	p = 0.0026 (Young > Old)
LPoCG/3/LPreCG/4	36	30	58	1296	-3.584	p = 0.0017 (Young > Old)
LPCUN/7/LSPL	12	54	46	1296	-3.800	p < 0.001 (Young > Old)
LSTG/22/42	66	36	16	864	-3.523	p = 0.0019 (Young > Old)
RFFG/20/RITG	-54	6	-26	648	-3.735	p = 0.0011 (Young > Old)
RMFG/11/RIFG	-36	-36	-14	648	-3.233	p = 0.0038 (Young > Old)
RITG/37/RMTG/20	-48	42	-8	648	-3.880	p < 0.001 (Young > Old)
LLING/17/18	0	72	-8	648	-3.349	p = 0.0029 (Young > Old)
RLING/RCUN/17/18	-18	78	4	432	-3.004	p = 0.0065 (Young > Old)
LPoCG/40/LSTG/41/42	54	24	16	432	-3.530	p = 0.0019 (Young > Old)
(c)						
LFFG/LITG/20	48	18	-26	7776	-4.934	p < 0.001 (Young > Old)
RFFG/RITG/20	-48	12	-26	2160	-4.109	p < 0.001 (Young > Old)
LINS/13/LSTG/41	36	24	16	1944	-3.710	p = 0.0012 (Young > Old)
RFFG/RLING/17/18	-24	78	-14	1728	-4.264	p < 0.001 (Young > Old)
LIFG/47 (medial)	24	-18	-20	864	-3.795	p < 0.001 (Young > Old)
LFFG/37	36	54	-8	864	-3.599	p = 0.0016 (Young > Old)
RHIP/RPHG/RAMYG	-18	6	-20	432	-2.992	p = 0.0067 (Young > Old)
LPCG/30 (lateral)	18	60	10	432	-3.285	p = 0.0034 (Young > Old)
LPCG/30/LCUN (medial)	6	66	10	432	-3.092	p = 0.0053 (Young> Old)

*Cluster extends rostromedially to include LACG

Region	Abbreviation	Region	Abbreviation
Amygdala	AMYG	Middle Occipital Gyrus	MOG
Anterior Cingulate Gyrus	ACG	Middle Temporal Gyrus	MTG
Cuneus	CUN	Posterior Cingulate Gyrus	PCG
Fusiform Gyrus	FFG	Precuneus	PCUN
Hippocampus	HIP	Parahippocampal Gyrus	PHG
Inferior Frontal Gyrus	IFG	Postcentral Gyrus	PoCG
Insular Cortex	INS	Precentral Gyrus	PreCG
Inferior Parietal Lobule	IPL	Supramarginal Gyrus	SMG
Inferior Temporal Gyrus	ITG	Superior Parietal Lobule	SPL
Lingual Gyrus	LING	Superior Temporal Gyrus	STG

+ Corresponding author (john-sheppard@northwestern.edu)
* Faculty sponsor (pwong@northwestern.edu)